Analytical and Bioanalytical Chemistry (2020) 412:8003–8014
https://doi.org/10.1007/s00216-020-02933-w

RESEARCH PAPER

Exercise-induced recovery of plasma lipids perturbed by ageing with nanoflow UHPLC-ESI-MS/MS

Kang Uk Kim[1] · Kyeong Jin Yoon[2] · Suhong Park[2] · Jong Cheol Lee[1] · Hyo Youl Moon[2,3,4] · Myeong Hee Moon[1]

Received: 24 July 2020 / Revised: 26 August 2020 / Accepted: 31 August 2020 / Published online: 12 September 2020

Abstract

Daily physical exercise is an essential part of life and is required for remaining healthy; it enhances therapeutic efficacy in the elderly and prevents age-related diseases associated with lipid profile alterations, such as cardiovascular disease, diabetes mellitus, and dementia. To more efficiently analyse the lipid profiles and unveil the effect of exercise in aged mice, we optimized our study by examining the effects of using ionization modifiers in the mobile phase and in-source fragmentation of lysophospholipids on the simultaneous analysis of fatty acids (FAs) including hydroxyl fatty acids, glycerophospholipids, sphingolipids, and glycerolipids using nanoflow ultrahigh performance liquid chromatography–electrospray ionization–tandem mass spectrometry. We applied the optimization to investigate the lipidomic plasma alterations in young (7 weeks old) and aged (84 weeks old) mice (C57BL/6) subjected to treadmill exercise. Of the 390 identified lipid species, 159 were quantified to investigate ageing-related lipid species responsive to physical exercise. In particular, circulating lysophosphatidylcholine and lysophosphatidylethanolamine levels showed a significant decrease, and lysophosphatidic acid showed a simultaneous increase with ageing. The saturated FA (16:0 and 18:0) increased with ageing while the unsaturated FA 22:6 decreased. Dihydroxy fatty acid (18:1_2OH) showed an exercise-induced recovery against ageing. It is notable that the levels of five triacylglycerol species significantly increased by as much as threefold with ageing, but their levels largely recovered to those observed in the young mice after exercise. These findings can help understand the influence of ageing on lipid perturbation and the role of physical exercise on lipidomic recovery in response to ageing-associated loss of physical status.

Keywords Plasma lipids · Physical exercise · Ageing effect · Mouse · nUHPLC-ESI-MS/MS

Abbreviations

AF	Ammonium formate
AH	Ammonium hydroxide
ANOVA	Analysis of variance
BEH	Ethylene bridged hybrid
BPC	Base peak chromatogram
Cer	Ceramide
CID	Collision-induced dissociation
CL	Cardiolipin
CVD	Cardiovascular diseases
DG	Diacylglycerol
DHFA	Dihydroxy fatty acid
EIC	Extracted ion chromatogram
FA	Fatty acid
GC-MS	Gas chromatography-mass spectrometry
GL	Glycerolipid
GPL	Glycerophospholipid
HexCer	Monohexosylceramide
HFA	Hydroxyl fatty acid
IS	Internal standard
ISF	In-source fragmentation

Electronic supplementary material The online version of this article (https://doi.org/10.1007/s00216-020-02933-w) contains supplementary material, which is available to authorized users.

✉ Hyo Youl Moon
skyman19@snu.ac.kr

✉ Myeong Hee Moon
mhmoon@yonsei.ac.kr

[1] Department of Chemistry, Yonsei University, Seodaemun-gu, Seoul 03722, South Korea

[2] Department of Physical Education, Seoul National University, Gwanak-gu, Seoul 08826, South Korea

[3] Institute of Sport Science, Seoul National University, Gwanak-gu, Seoul 08826, South Korea

[4] Institute on Ageing, Seoul National University, Seoul 08826, South Korea

LOD	Limit of detection
LOQ	Limit of quantitation
LPA	Lysophosphatidic acid
LPC	Lysophosphatidylcholine
LPE	Lysophosphatidylethanolamine
LPG	Lysophosphatidylglycerol
LPI	Lysophosphatidylinositol
LPL	Lysophospholipid
LPS	Lysophosphatidylserine
MHFA	Monohydroxy fatty acid
MRS	Magnetic resonance spectroscopy
MTBE	Methyl-*tert*-butyl ether
MUFA	Monounsaturated fatty acid
nUHPLC-ESI-MS/MS	Nanoflow ultrahigh performance liquid chromatography–electrospray ionization–tandem mass spectrometry
PC	Phosphatidylcholine
PCA	Principal component analysis
PCp	Phosphatidylcholine plasmalogen
PE	Phosphatidylethanolamine
PEp	Phosphatidylethanolamine plasmalogen
PG	Phosphatidylglycerol
PI	Phosphatidylinositol
PS	Phosphatidylserine
PUFA	Polyunsaturated fatty acid
SFA	Saturated fatty acid
SL	Sphingolipid
SM	Sphingomyelin
SRM	Selected reaction monitoring
SulfoHexCer	Sulfatide
T2D	Type 2 diabetes
TG	Triacylglycerol

Introduction

As the human life expectancy increases with advances in the field of life science, it is increasingly important to expand the healthspan, a healthy life expectancy, with the absence of chronic diseases especially among older people. While numerous efforts are continuously being made to promote health-related quality of life including early disease diagnosis and prevention, daily physical exercise has been recognized as an essential part of life for remaining healthy by preventing the occurrence of age-related diseases like cardiovascular disease and diabetes [1, 2], postponing the onset of dementia [3], and enhancing the therapeutic effects before and after major surgery [4]. As age-induced phenomenon like immune function decline [5], loss of muscle mass [6], and increased risk of insulin resistance, obesity, and cardiovascular disease [7] are reportedly related to the alterations in lipid profile, the effect of physical exercise on lipid control in metabolism has gained much attention. Lipids are the major components of biological membranes, but their roles are essential including energy storage, signal transduction between cells, cell proliferation, and apoptosis [8, 9]. Among various lipid classes, triacylglycerol (TG) levels reportedly increase in muscle tissues with ageing, and TG accumulation is associated with insulin resistance [10, 11] or cardiovascular diseases [12, 13]. However, studies reported that aerobic exercise significantly lowered blood TG, cholesterol [14], and plasma ceramide (Cer) levels, especially saturated Cer 14:0 which is closely associated with improved insulin sensitivity [15]. An age-induced increase of palmitate (C16:0), the most abundant circulating saturated fatty acid (FA)—related to decreased insulin sensitivity—is associated with decreased muscle mass as it decreased myotube size [16]. Moreover, monounsaturated fatty acids (MUFAs) and polyunsaturated fatty acids (PUFAs) reportedly prevent palmitate-induced accumulation of diacylglycerols (DG) containing saturated fatty acyl chains (18:0 and 20:0), which promote insulin resistance.

Lipids are classified into eight different categories including glycerophospholipids (GPL), glycerolipids (GL), sphingolipids (SLs), fatty acyls, sterols, saccharolipids, prenols, and polyketides [17]. Lipid analysis often requires a systematic characterization of lipid molecular structures followed by quantification based on mass spectrometry (MS). Chromatographic separation before MS is required due to the complicated nature of lipid molecular structures that vary with respect to polar head groups, the degree of unsaturation, and length of acyl chain. In the case of FAs, gas chromatography (GC)–MS has been widely utilized as it provides high-speed separation with enhanced detection capability compared with LC-MS [18–22]. However, FA analysis with GC-MS requires a derivatization of FA into volatile compounds like fatty acid methyl esters. Moreover, it is not possible to analyse other polar lipids together with FA using GC-MS in a single run. For analysing biological and pathological influences on lipid perturbation, a comprehensive analytical platform must be developed to ensure consistent sample preparation and analysis. Liquid chromatography coupled to electrospray ionization–tandem MS (LC-ESI-MS/MS) is commonly utilized to analyse most polar lipids in their intact forms. As nanoflow LC offers improved separation efficiency and detection capability along with the requirement of a reduced sample injection amount when combined with ESI-MS/MS [23], it can serve as a powerful tool for global and targeted quantitative lipidomic analyses. In our laboratory, nanoflow ultrahigh performance LC (nUHPLC)-ESI-MS/MS has been utilized to study lipidomic perturbations in plasma from patients with Alzheimer's diseases and mild cognitive impairments [24], brain tissues of mice with high-fat diet [25], and in urinary exosomes from patients with prostate cancer [26].

Here, optimization was accomplished first by investigating the effects of ionization modifiers in the mobile phase and in-source fragmentation of lysophospholipids (LPLs) on the

simultaneous analysis of FAs including hydroxyl fatty acids (HFAs) with GPLs, SLs, and GLs using nUHPLC-ESI-MS/MS. As FAs and LPLs have similar polarities, resulting in co-elution in reversed phase LC, FA anions must be distinguished from the possible fatty acyl fragment ions produced from LPLs having a common acyl chain structure via in-source fragmentation during ESI. Next, our protocol was applied to investigate the lipidomic alterations in mice plasma from both young (7 weeks old) and aged (84 weeks old) mouse (C57BL/6) groups that were subjected to a treadmill exercise for a period of 3 weeks compared with mouse groups without exercise. Plasma lipids from each group (young and aged) were comprehensively analysed using non-targeted identification of lipid molecular structures followed by targeted quantification compared with each control group. Exercise-induced changes in individual lipid profiles perturbed by ageing were statistically examined to assess lipidomic signatures in the form of the exercise-responsive lipids in response to ageing.

Materials and methods

Reagents

The following lipid standards were purchased from Avanti Polar Lipids Inc. (Alabaster, AL, USA) and Matreya, LLC. (Pleasant Gap, PA, USA). A total of 34 lipid standards were used to optimize the nUHPLC-ESI-MS/MS run conditions, fatty acid (FA) 14:0, FA 15:0, FA 16:0, FA 18:2, FA 20:0, FA 20:4, FA 22:6, monohydroxy FA (MHFA) 14:0 (2OH), MHFA 22:6 (17OH), dihydroxy FA (DHFA) 20:4 (5OH, 12OH), lysophosphatidic acid (LPA) 18:0, phosphatidic acid (PA) 14:0/14:0, lysophosphatidylglycerol (LPG) 14:0, LPG 18:0, phosphatidylglycerol (PG) 14:0/14:0, lysophosphatidylinositol (LPI) 18:0, phosphatidylinositol (PI) 18:0/20:4, lysophosphatidylserine (LPS) 18:1, LPS 17:1, phosphatidylserine (PS) 14:0/14:0, lysophosphatidylcholine (LPC) 16:0, phosphatidylcholine (PC) 18:0/18:1, PC plasmalogen (PCp) P-18:0/22:6, lysophosphatidylethanolamine (LPE) 16:0, LPE 18:0, phosphatidylethanolamine (PE) 12:0/12:0, PE 16:0/16:0, PE plasmalogen (PEp) P-18:0/22:6, ceramide (Cer) d18:1/22:0, sphingomyelin (SM) d18:1/16:0, monohexosylceramide (HexCer) d18:1/12:0, sulfatide (SulfoHexCer) d18:1/24:0, diacylglycerol (DG) 16:0/18:1, triacylglycerol (TG) 18:1/18:1/18:1, and cardiolipin (CL) 14:0/14:0/14:0/14:0. The following 14 lipid standards with odd-numbered or deuterated fatty acyl chains as non-endogenous lipids were added to lipid extracts as internal standards for targeted quantitative analysis, FA 15:0, LPA 17:1, LPG 13:0, LPI 13:0, PI 15:0/18:1(d7), LPC 18:1(d7), PC 15:0/18:1(d7), LPE 18:1(d7), PE 15:0/18:1(d7), Cer d18:1(d7)/24:0, SM d18:1/18:1(d9), HexCer d18:1(d7)/15:0, DG 15:0/18:1(d7), and TG 15:0/18:1(d7)/15:0. The following 16 lipid standards were spiked into lipid extracts as external standards along with internal standards to establish calibration curves to calculate limit of detection (LOD) and limit of quantitation (LOQ), FA 19:0, LPA 17:0, LPG 17:1, LPI 17:1, PI 16:0(d31)/18:1, LPC 17:1, PC 17:0/17:0, PC P-18:0/18:1(d9), LPE 17:1, PE 17:0/17:0, PE P-18:0/18:1(d9), Cer d18:1(d7)/24:1, SM d18:1/17:0, HexCer d18:1/17:0, D_5-DG 18:0/18:0, and D_5-TG 17:0/17:1/17:0. Methyl-*tert*-butyl ether (MTBE) and HPLC grade solvents including water, methanol, isopropanol, and acetonitrile were purchased from Avantor, Inc. (Center Valley, PA, USA). Ammonium hydroxide (AH) and ammonium formate (AF) used as LC solvent ionization modifiers were purchased from Sigma-Aldrich (St. Louis, MO, USA). Fused silica capillary tubes with inner diameters of 20, 50, and 100 μm and an outer diameter of 360 μm were purchased from Polymicro Technology, LLC (Phoenix, AZ, USA). Watchers® ODS-P C-18 particles (3 μm and 100 Å) from Isu Industry Corp. (Seoul, Korea) and ethylene bridged hybrid (BEH) particles (1.7 μm) unpacked from ACQUITY UPLC® BEH C18 column (2.1 mm × 100 mm) of Waters™ (Milford, MA, USA) were used as packing materials for analytical reverse phase LC columns.

Animals and physical exercise

The two groups of C57/BL6 male mice, 7-week-old mice (young group, $n = 11$) and 84-week-old mice (aged group, $n = 10$), were purchased from Korea Research Institute of Bioscience and Biotechnology (KRIBB), Daejeon, Korea. Mice in each group were randomly divided into a sedentary group (control) and an exercise group and housed in standard conditions with food and water ad libitum, young control (YC, $n = 6$), young with exercise (YX, $n = 5$), aged control (AC, $n = 5$), and aged with exercise (AX, $n = 5$). Exercise was performed using a treadmill for 3 weeks, with two sessions (30 min each) per day and 5 days a week. Mice in each exercise group were adapted to and familiarized with treadmill for 3 days at various speeds (15 min/session at a 0 m/min for 3 min, 5 m/min for 2 min, and 8 m/min for 10 min). Two sessions of treadmill training were provided each day. At each session, mice began with 3-min of warm-up running at three consecutive speeds (5, 8, and 10 m/min for 1 min each). Next, the speed was ramped up to 12 m/min and maintained for 30 min. The training speed was increased by 2 m/min at every week and resumed to 5 m/min for 2 min to cool down. After a 1-h break, the second training session was performed with the same protocol.

Body fat and lean body masses were measured by using magnetic resonance spectroscopy (MRS) with a Minispec LF-50 from Bruker BioSpin (Billerica, MA, USA) at 24-h after the last exercise session. Average body weight, body fat, and glucose levels are listed for each group in Table S1 of the Electronic Supplementary Material (ESM).

Blood samples were collected after the scheduled experiments for all groups. Plasma sample was collected in a heparin-treated tube using cardiac puncture during deep anaesthesia with isofluorane (Henry Schein Animal Health, OH) and O_2, centrifuged at 2500 rpm for 15 min, and stored at − 80 °C until lipid analysis. Animals were maintained in accordance with the National Institutes of Health guidelines. Animal experiments were approved by the Institutional Animal Care and Use Committee of Seoul National University (SNU-171226-3).

Lipid extraction

For the identification of lipid molecular structures, the same amount of plasma sample from each mouse was pooled to a total volume of 25 μL for each mouse group. For lipid quantification, 25 μL of an individual plasma sample added with internal standards was used. Plasma samples were dried first under N_2 gas using an Evatros Mini evaporator from Goojung Engineering (Seoul, Korea). Dried plasma samples were extracted with MTBE/methanol according to a previous protocol [27]. Briefly, each dried lipid sample was mixed with 300 μL of methanol and incubated for 10 min in an ice bath. One thousand microlitres of MTBE was added to the mixture, the mixture was vortexed for 1 h, and 250 μL of water was added before incubating for another 10 min. The mixture was centrifuged at 1000*g* for 10 min, and the organic supernatant was transferred to another centrifuge tube. The remaining aqueous layer was mixed with 300 μL of MTBE and vortexed for 10 min. Mixtures were tip-sonicated for 2 min and centrifugated at 1000*g* for 10 min. The resulting organic layer was removed to merge with the previously collected organic layer. The organic solution containing lipid extracts was dried under N_2 using an evaporator. Dried lipid extracts were reconstituted in 200 μL of chloroform:methanol (1:9, v/v) and stored at − 80 °C. The stored lipid extracts were diluted with 200 μL of water:methanol (1:9, v/v) before nUHPLC-ESI-MS/MS analysis.

nUHPLC-ESI-MS/MS analysis

Here, two sets of nUHPLC-ESI-MS/MS systems were employed for lipid analysis, a Dionex Ultimate 3000 RSLCnano system with LTQ Velos ion trap mass spectrometer from Thermo Fisher Scientific (San Jose, CA, USA) for non-targeted lipid identification and a nanoACQUITY UPLC system from Waters™ (Milford, MA, USA) coupled with a TSQ Vantage triple-stage quadrupole mass spectrometer system from Thermo Fisher Scientific for targeted lipid quantification based on selected reaction monitoring (SRM) method. Reversed phase capillary LC columns were prepared in the laboratory using a 100 μm-I.D. fused silica capillary by fabricating a pulled-tip end and packing with Watchers® ODS-P C-18 particles (3 μm and 100 Å) for a 5 mm portion of the tip followed by packing the rest (7 cm) with 1.7-μm ACQUITY UPLC BEH resin under nitrogen gas at 1000 psi. The column to the nUHPLC system and ESI-MS were connected using the same procedure as described elsewhere. nUHPLC separation of lipids was done with binary gradient elution using water:acetonitrile (9:1, v/v) for mobile phase A and acetonitrile:methanol:isopropanol (2:2:6, v/v) for mobile phase B. To optimize a run condition for the simultaneous analysis of FAs with other lipid classes, ionization modifiers were tested by varying the AF concentration in 0.05% AH. ESI voltages of 3 kV in the positive ion mode and 1.5 kV in negative ion mode were used at a heated ion transfer tube temperature of 350 °C.

The pooled lipid extract sample of each group was used for global lipid identification. One microlitre of each extract was injected into the capillary column via autosampler using mobile phase A at a flow rate of 1.0 μL/min for 7.5 min. After loading the sample, the pump flow rate was changed to 10.0 μL/min at split mode and the final column flow rate was adjusted to 300 nL/min. Gradient elution began with 60% of the mobile phase B; this was increased to 70% for 10 min, to 100% for 17.5 min, maintained at 100% for 12.5 min, and resumed to 0%. Re-equilibration of the analytical column was conducted for 10 min. Data-dependent collision-induced dissociation (CID) experiments were performed with 40% normalized collision energy. The lipid molecular structures were identified using LiPilot software, a PC-based software developed in our laboratory [28].

For targeted lipid quantification, individual lipid extract samples spiked with internal standards were analysed by injecting 1 μL of each extract using the same analytical column employed during global identification. The sample loading was done with mobile phase A at a flow rate of 1.0 μL/min for 7.5 min. The valve was switched for sample elution in split mode, and the pump flow rate was changed to 15.0 μL/min. However, the column flow rate was adjusted to 300 nL/min by applying a pressure tube at the split end. Gradient elution began at 60% of the mobile phase B; this was increased to 70% for 3 min, 90% for 12 min, and further to 100% for 5 min. It was resumed to 0% after another 5 min of column washing at 100% B. During SRM quantification, the polarity switching mode was utilized to alternatively detect the lipid ion in positive and negative ion modes, LPC, PC, PCp, LPE, PE, PEp, Cer, SM, HexCer, DG, and TG were detected in positive ion mode, and FA, MHFA, DHFA, LPA, LPG, LPI, and PI were detected in the negative ion mode. Types of precursor and product ions and the collision energy value assigned for each lipid class type used for SRM quantification are listed in Table S2 (see ESM). The quantified amount of each lipid species was calculated as the corrected peak area, the ratio of the peak area of a species to the area of the IS specific to each lipid class, and it was converted to a pmol/μL

amount using the calibration curve. In the case of FA from plastics like tubes and micro tips that could interfere with FA analysis, endogenous FA signals were corrected by computationally removing the exogenous FA signal [29, 30].

Two-way analysis of variance (ANOVA) was utilized to analyse the data and simultaneously evaluate the ageing and/or exercising effects of the four mouse groups. Post hoc analysis was conducted using a Bonferroni test with SPSS software (version 20.0, IBM Corp., Armonk, NY, USA). All data were log-transformed prior to statistical analysis. Principal component analysis (PCA) was performed using Minitab 17 software.

Results

Effect of ionization modifiers on simultaneous analysis of FAs with other lipid classes

Targeted lipid quantitation using nUHPLC-ESI-MS/MS can be facilitated using polarity switching methods in which lipid detection alternates between positive and negative ion MS modes. The polarity switching lipid analysis decreases the analysis time without running the same sample separately in both ion modes. However, a suitable type of mixed ionization modifier that can ionize lipid molecules in either the positive or negative ions is necessary. For simultaneous analysis of FAs with other lipid classes in blood plasma using nUHPLC-ESI-MS/MS with the polarity switching method, the ionization efficiencies of FAs and other lipids must be investigated by varying the composition of ionization modifiers. Figure S1 (see ESM) shows the variation of MS intensities for 17 lipid classes including four FAs by varying the composition of ammonium formate (AF) at a fixed (0.05%) ammonium hydroxide (AH) concentration. While MS intensities of anionic lipids like FA, PS, PG, PI, PA, and CL that were monitored in the negative ion mode used to be most effective with 0.05% AH alone, the MS intensities of neutral polar lipids including PC, PE, and TG in positive ion mode were relatively poor. The addition of 5 mM AF to AH enhanced neutral polar lipid ionization, but it deteriorated the ionization of anionic lipids. For the efficient ionization of both anionic and neutral polar lipids, 0.5 mM AF added to 0.05% AH was selected as an optimum concentration that can be applied for simultaneous analysis of all lipids including FAs. Figure S2 (see ESM) shows the base peak chromatograms (BPCs) of standard lipid mixtures for which run conditions were used for structural determination of lipids from mouse plasma samples in both positive and negative nUHPLC-ESI-MS/MS ion modes, separately.

Characterization of FA along with other lipid classes using nUHPLC-ESI-MS/MS

When FA and LPG with a common acyl chain in a lipidome sample are analysed using RPLC, their retention times can be similar. In this case, there is a chance to detect the FA precursor ion ($[M-H]^-$) simultaneously with the fatty carboxylate fragment ions ($[RCOO]^-$) produced by in-source fragmentation of LPG during ESI. Therefore, the degree of in-source fragmentation of LPG was investigated using lipid standards of LPG 14:0 and FA 14:0. Figure 1a shows the extracted ion chromatogram (EICs) of LPG 14:0 (m/z 455.3, $t_r = 4.48$ min) and PG 14:0/14:0 (m/z 665.4, $t_r = 20.25$ min) as forms of $[M-H]^-$ in the top chromatogram which was compared with the EIC of m/z 227.3 showing the detection of $[M-H]^-$ ions of FA 14:0 at 4.22 min and $[RCOO]^-$ ions at 4.48 min produced from the in-source fragmentation of LPG 14:0, which were resolved based on retention times. The calculated peak area of $[RCOO]^-$ ions from LPG 14:0 was 0.7% compared with that for LPG 14:0—which can be negligible—for quantifying FAs together with other lipids. As SRM-based quantitation was performed here with triple quadrupole MS while data-dependent CID experiments for the global identification of lipids were performed with ion trap MS, a similar investigation was made at an even elongated gradient run condition with triple quadrupole MS to separate FA 14:0 and LPG 14:0, and the corresponding EICs in Fig. 1b demonstrated a complete separation of the two regioisomers (the first peak for LPG with the acyl chain located at sn-2 position and the last tall peak at sn-1 position) of LPG 14:0 at the top chromatogram, demonstrating the resolving power of the home-made nUHPLC column employed here. However, $[RCOO]^-$ fragment ions from LPG 14:0 were not observed in the bottom extracted chromatogram of Fig. 1b based on m/z 227.3. Further ISF investigation from other lysophospholipids (LPLs) showed that acyl carboxylate fragment ions were not detected from LPI 18:0, LPA 18:0, and LPS 17:1 as shown in Fig. S3 (see ESM).

Non-targeted identification and SRM-based lipid quantification

Lipid structure was determined using pooled plasma samples (one pooled sample from both control groups and the other from both exercise groups), and their BPCs are shown in Fig. S4 (see ESM). A total of 390 lipids including 20 FAs and 17 HFAs were identified from the pooled plasma samples based on MS/MS spectra obtained using data-dependent collision-induced dissociation experiments based on ion trap MS of nUHPLC-ESI-MS/MS. Among 390 lipid species, SRM-based quantification was accomplished for 159 lipid species using triple quadrupole MS interfaced with nUHPLC because lipid species below the limit of quantitation (LOQ) were

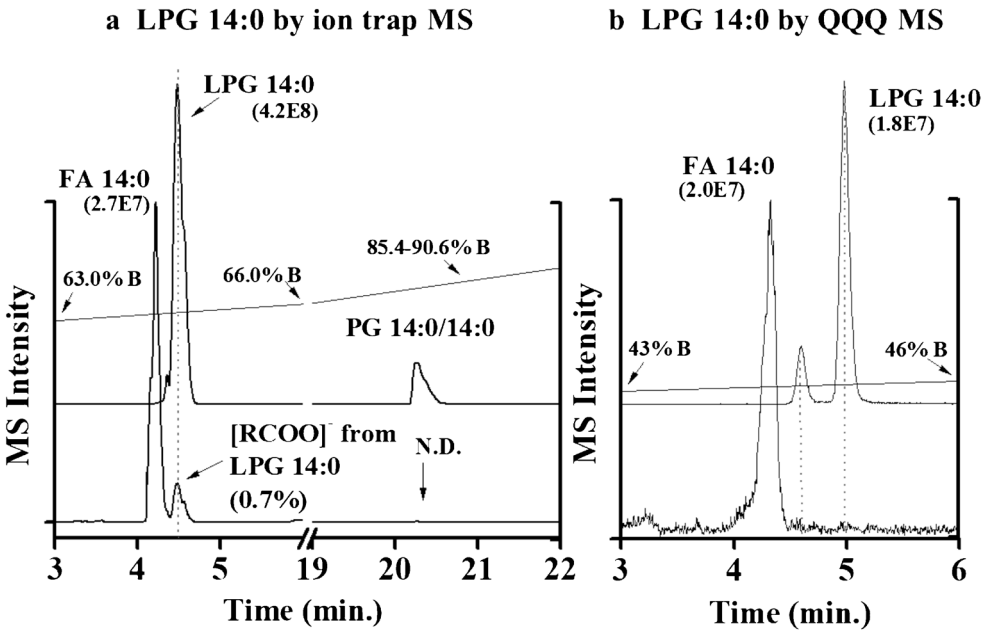

Fig. 1 **a** Extracted ion chromatogram (EIC) of LPG 14:0 (m/z 455.3, t_r = 4.48 min) and PG 14:0/14:0 (m/z 665.4, t_r = 20.25 min) as $[M\text{-}H]^-$ ion forms (top) and EIC of m/z 227.3 showing $[M\text{-}H]^-$ ions of FA 14:0 (t_r = 4.22 min) and $[RCOO]^-$ fragment ions (t_r = 4.48 min) (bottom) produced by the fragmentation of LPG 14:0 during ESI in the negative ion mode of nUHPLC-ESI-MS/MS (ion trap) and **b** EICs of LPG 14:0 (top) and m/z 227.3 (bottom, showing FA 14:0 and no fragment ions) using nUHPLC-ESI-MS/MS (QQQ)

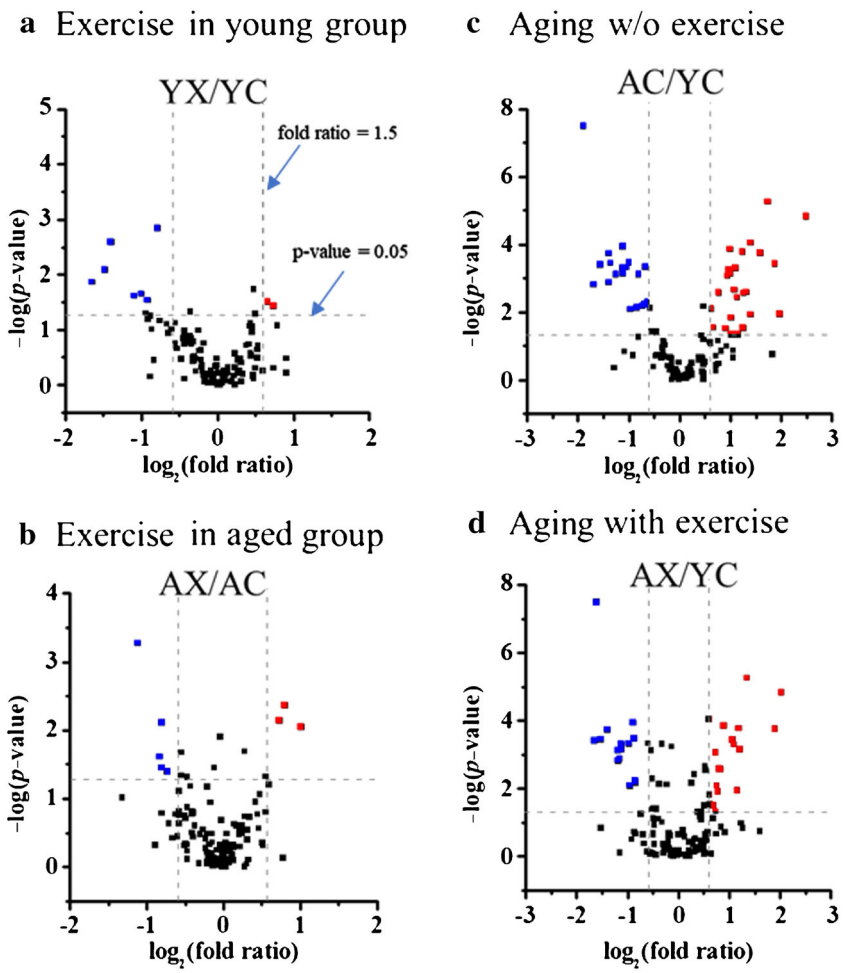

Fig. 2 Volcano plots of quantified lipid species showing exercise effects in **a** young and **b** aged groups and ageing effects **c** without exercise and **d** with exercise. The acronyms A, Y, C, and X represent aged, young, control, and exercise, respectively

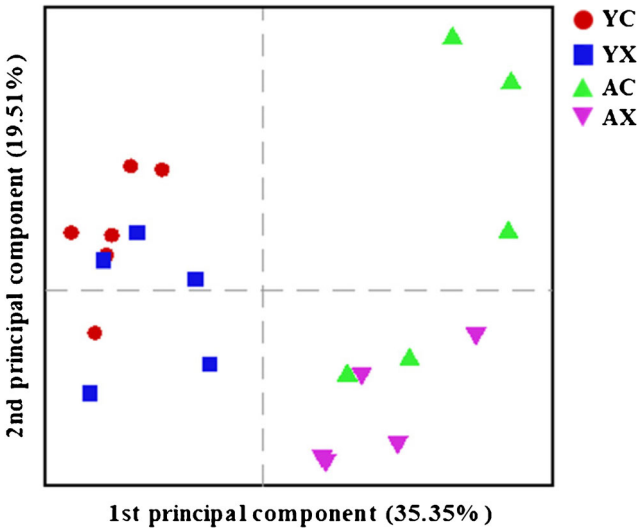

Fig. 3 Principal component analysis (PCA) plots showing differences in lipid profiles between 4 mice groups. The acronyms A, Y, C, and X represent aged, young, control, and exercise, respectively. Plots are based on lipid species showing statistical main effect of ageing and/or exercise, or interaction effect between ageing and exercise (p value < 0.05)

excluded and lipids in the classes of PC, PE, and TG were quantified based on the total length and number of double bonds in their acyl chains. The limit of detection (LOD)/LOQ values ranged from 0.006/0.021 pmol for SM 18:0/18:0 D5 in the linear concentration range of 1–500 fmol to 0.078/0.260 pmol for LPA 17:0 in the range of 1–1000 fmol. Detailed LOD/LOQ values of the sixteen lipid classes are listed in Table S3 (see ESM) and the calibration curves in Fig. S5 (see ESM). Quantified results of individual lipid species of the four mouse groups are listed in Table S4 (see ESM) represented by the normalized lipid amount (pmol/μL) along with the relative abundance values in each lipid class. Detailed information on acyl chain structures of PC, PE, and TG is listed in Table S5 (see ESM).

Effect of ageing and exercise on mouse plasma lipid profiles

Alterations in individual lipid amounts among the four mouse groups were represented using Volcano plots (−log (p value) vs. $\log_2$ (fold ratio) in Fig. 2), which illustrated the exercise effect in the (a) young group (fold ratio of YX/YC) and (b) aged group (AX/AC) and the ageing effect (c) without exercise (AC/YC) and (d) with exercise (AX/YC). Vertical lines in the Volcano plot represent a 1.5-fold decrease (left) and increase (right), and the horizontal line is equivalent to a p value of 0.05. It appears that only a few species show significant changes after exercise in both young (plot a) and aged (b) groups. However, a number of species showed significant increases or decreases (> 1.5-fold and $p < 0.05$) after ageing without exercise (plot c), but their numbers were significantly decreased after exercise (plot d) in the aged group (vs. YC). This represents that the effect of exercise on the change in lipid profiles is larger in the ageing group than in the young group. This implies that ageing-induced changes were decreased by exercise. Ageing effect between the two exercise groups (AX vs. YX) is compared in Fig. S6 (see ESM), showing that the ageing effect in the exercise groups is less serious than those without exercise. Differences in the overall lipid profiles were examined using principal component analysis (PCA) based on lipid species showing a prominent effect ($p < 0.05$) on ageing and/or exercise and statistical interaction between ageing and exercise in Fig. 3. The PCA plot shows that the difference in lipid profiles after ageing is obvious as data points of the aged groups (both AC and AX) clustered apart from those of the young groups. In addition, the exercise

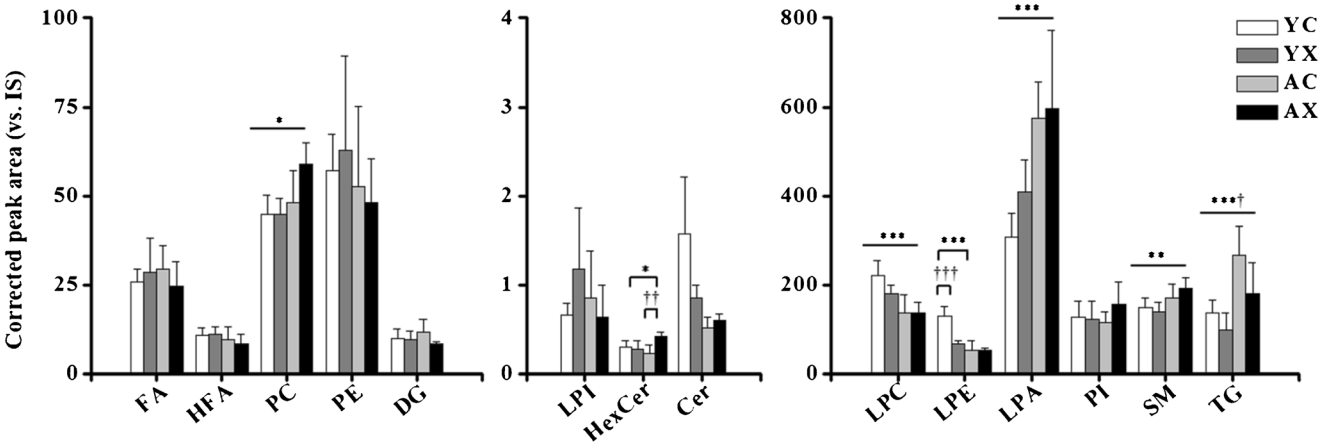

Fig. 4 Total amount (based on corrected peak area relative to IS) of all lipids in each lipid class showing ageing and/or exercising effects: ∗ for $p < 0.05$, ∗∗ for $p < 0.01$, and ∗∗∗ for $p < 0.001$ exhibiting ageing effect; † for $p < 0.05$, †† for $p < 0.01$, and ††† for $p < 0.001$ exhibiting exercising effect. Straight lines above bar graphs represent the main effect of ageing or exercising and lines with sticks represent an interaction effect between ageing and exercising effects (A aged, Y young, C control, and X exercise)

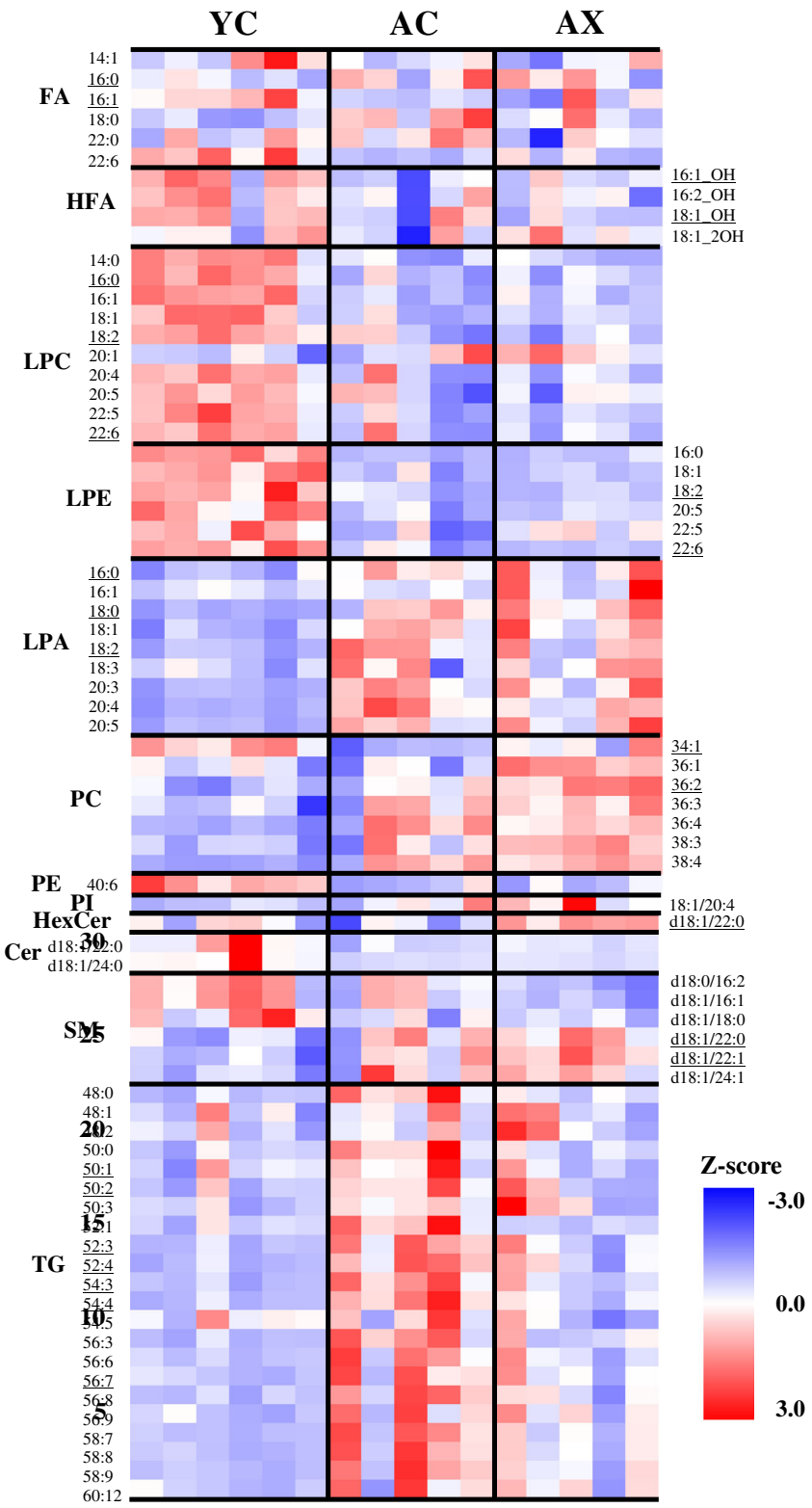

Fig. 5 Heat map of lipid species showing significant changes ($p < 0.05$ by two-way ANOVA) in the AC and AX groups compared with YC. Underlined species represent high abundance species in each lipid class

effect was larger in the ageing groups than in the young groups.

Figure 4 shows the differences in the total lipid amount of each lipid class among the four mouse groups expressed with the corrected peak area relative to the peak area of each internal standard. Concentrations of internal standards spiked to lipid extract sample were 25 to 675 fmol/μL as listed in Table S3 (see ESM), and 1 μL of the internal standard mixture

Table 1 Lipid species showing exercise effect alone and exercise-induced recovery against ageing with statistical significance

Class	Acyl chain	AC/YC			AX/AC		
		Fold ratio	*p* value	Trend	Fold ratio	*p* value	Trend
FA	22:0	1.15 ± 0.23	0.415	–	0.72 ± 0.19	0.048	↓
	18:1_2OH	0.80 ± 0.11	0.166	–	1.33 ± 0.20	0.011	↑
PC	36:2	1.24 ± 0.05	0.053	–	1.34 ± 0.05	0.013	↑
TG	48:0	2.65 ± 0.26	< 0.001	↑	0.57 ± 0.06	0.008	↓
	52:4	2.03 ± 0.14	0.015	↑	0.75 ± 0.05	0.012	↓
	54:4	2.41 ± 0.18	0.003	↑	0.60 ± 0.04	0.040	↓
	56:3	3.69 ± 0.49	< 0.001	↑	0.57 ± 0.07	0.035	↓
	58:7	3.93 ± 1.09	0.012	↑	0.57 ± 0.10	0.018	↓
LPE	22:5	0.48 ± 0.14	< 0.001	↓	1.66 ± 0.53	0.007	↑

was included in each nUHPLC-ESI-MS/MS run injection. Lipid classes showing a significant change ($p < 0.05$) among the four groups were marked with * and † along with the different type of lines (straight line for ageing or exercising effect and a line with sticks for an interaction effect between ageing and exercising effects) above the bar graph. Among lipid classes, LPC and LPE tended to decrease with ageing, while PC, LPA, SM, and TG increase with ageing. Moreover, LPE showed exercise-induced decrease in the young group, and TG decreased after exercise in both the young and ageing groups. PC, LPC, SM, and TG exhibited the main effect either in exercise or ageing based on statistical analysis, and HexCer and LPE showed the interaction effect between ageing and exercise. HexCer appeared to have no exercise effect in the young group and no ageing effect, but it exhibited an exercise effect in the ageing group. LPE showed an exercise effect only in the young group with an ageing effect. Lipid species showing significant difference ($p < 0.05$) in the AC and AX groups compared with YC were selected, and their relative amounts were illustrated using the heat map in Fig. 5. The heat map shows ageing-induced decreases in FA, HFA, LPC, and LPE species and increases in LPA, PC, and TG in the aged groups. However, it shows remarkable decreases in the levels of most TG species after exercise. Some individual lipid species of other classes showed recovery trends, too. This will be further investigated.

Alterations in individual lipid levels after ageing and exercise

The effect of ageing-/exercise-induced lipid perturbation was further examined with individual lipid species showing significant changes based on the two-way analysis of variance test. Subsequently, lipid species showing the main effect (ageing or exercise effect) and the interaction effect between ageing and exercise were plotted with the individual lipid amounts of the four mouse groups in Fig. S7 (see ESM). Next, lipids were classified into two categories: lipids with significant ageing effect alone without being influenced by exercise and lipids showing an exercise effect with or without being related to ageing effect in Figs. 6 and 7, respectively, with *p* values obtained by post hoc Bonferroni test analysis. While levels of five LPC (14:0, 16:0,

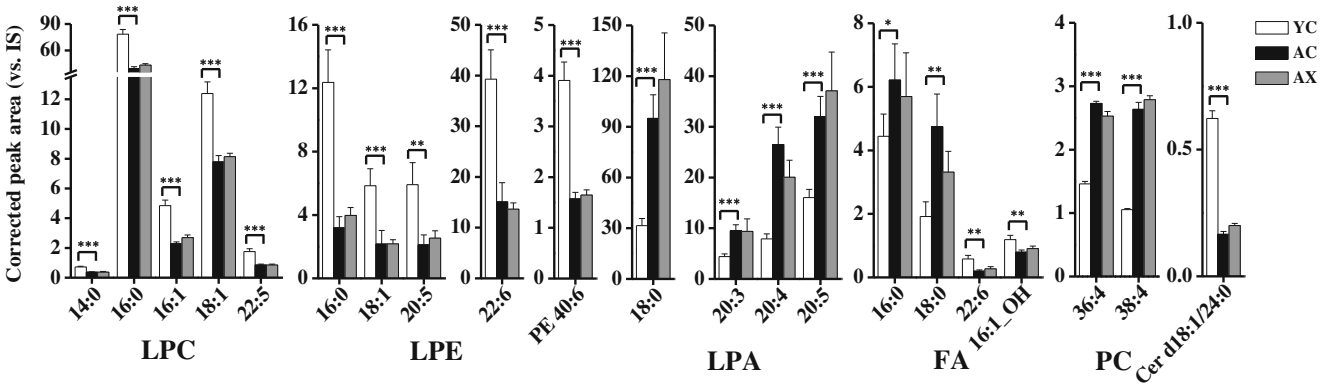

Fig. 6 Normalized peak area for lipid species (vs. internal standard) showing ageing effect only without exercise effect. The acronyms A, Y, C, and X represent aged, young, control, and exercise, respectively. Statistical significances of ∗, ∗∗, and ∗∗∗ represent for $p < 0.05$, $p < 0.01$ and $p < 0.001$, respectively

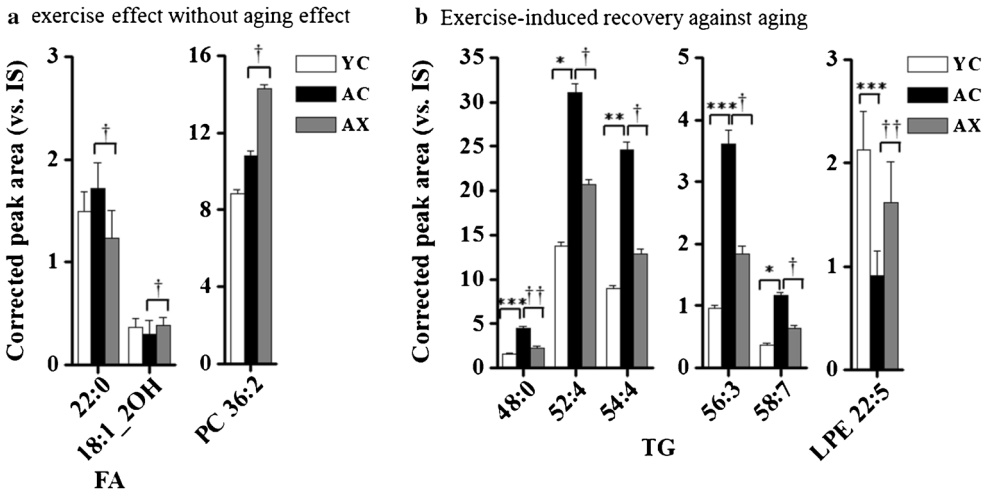

Fig. 7 Normalized peak area for lipid species showing **a** exercise effect without ageing effect and **b** exercise-induced recovery against ageing (A aged, Y young, C control, and X exercise) with statistical significance: ∗ for $p < 0.05$, ∗∗ for $p < 0.01$ and ∗∗∗ for $p < 0.001$ for ageing effect, and † for $p < 0.05$, †† for $p < 0.01$ and ††† for $p < 0.001$ for exercise effect

16:1, 18:1, and 22:5), four LPE (16:0, 18:1, 20:5, and 22:6), and PE 40:6 species were decreased after ageing, four LPA (18:0, 20:3, 20:4, and 20:5), two FA (16:0 and 18:0), and two PC (36:4 and 38:4) increased with ageing in Fig. 6. Figure 7a shows the lipid species (HFA 18:1_2OH and PC 36:2) exhibiting an exercise-induced increase in their levels without a significant influence by ageing except the decrease in FA 22:0. However, Fig. 7b shows five TG species representing significant increases after ageing followed by remarkable decreases after exercise; however, an opposite trend was observed in case of LPE 22:5. Data for these lipid species in Fig. 7 are listed in Table 1 expressed with the fold ratio values (AC/YC and AX/AC).

Discussion

Low plasma LPC levels indicate an ageing phenotype associated with an impairment of mitochondrial oxidative capacity in adults; this is related to the increase of insulin resistance and poor muscle quality in older adults [31, 32]. Ageing-associated changes in lipids were found with decreased LPC 16:0 and 16:1 along with an increased PC 38:4 in the mouse serum [33, 34], which agreed with our observations. While most LPE species showed two- to threefold decreases with ageing, they were not responsive to physical exercise except LPE 22:5 which showed a remarkable recovery toward the level observed in the young group after exercise. LPE and LPC levels reportedly decreased with metabolic diseases like type 2 diabetes (T2D), a phenomenon that is strongly associated with ageing [35], but little is known about its function. However, LPE is known to play a role in slowing cellular senescence in plants [36] and is known to inhibit phospholipase D, which increases its activity in ageing [37]. As LPE can also act as a signalling molecule [38], future study is required to determine the role of LPE 22:5 in ageing and exercise. LPC is also a precursor to LPA which is a platelet activator that is highly accumulated in atherosclerotic plaque. Therefore, LPA is known to be strongly associated with the progress of cardiovascular diseases like acute coronary syndrome, a significant risk factor to older age [39, 40]. A decrease in the levels of circulating LPC and LPE species and a simultaneous increase in LPA in the ageing group in our study showed that typical lipidomic alterations occurred in animals examined after ageing. However, physical exercise was not significantly effective at recovering the perturbed LPC, LPE, and LPA levels except for LPE 22:5.

In the case of FA, ageing increased the levels of saturated FA (16:0 and 18:0) species, but those of unsaturated FA 22:6 decreased. Studies on age-associated changes in FA showed that saturated FA elevation induced inflammation and metabolic disorders like insulin resistance, and FA 16:0, a major saturated FA, was reported to largely increase in the plasma of older human adults [41, 42] and patients with type 2 diabetes [43]. It was reported that long-chain SFAs like FA 16:0 or FA 18:0 induced cytotoxicity, but unsaturated FAs like arachidonic acid (FA 20:5) or docosahexaenoic acid (FA 22:6) prevented cytokine-induced cell death and promoted insulin secretion [44]. While FA levels in our study showed the same trends reported in the literature, the FA species in Fig. 6 did not significantly respond to physical exercise. However, HFAs show a similar trend upon ageing and exercise with relatively weak statistical evidence. While FA 16:1_OH showed an ageing-associated decrease but showed a weak recovery effect in response to physical exercise, FA 18:1_2OH showed an exercise-induced recovery although the influence on ageing was not significant. FA 16:1_OH and 18:1_2OH were relatively high abundance HFAs among the seventeen identified HFA species (ESM Table S4), but the amounts of the two HFA species were relatively small compared with those of other FAs. Therefore, it is not yet clear how to distinguish exercise-induced HFA recovery.

High TG level is a significant risk factor for metabolic diseases including T2D, cardiovascular diseases (CVD), and obesity, phenomena that are frequently observed in elderly people [45, 46]. Exercise-induced decreases in circulating

TG levels have been reported in a number of studies involving athletes after marathon running and diabetic patients with exercise [47, 48]. It was also reported that sarcopenic obesity may increase the risk of CVD more than simple obesity due to the increased levels of several TG species [49]. The increased serum TG level in sarcopenic obesity was decreased by aerobic and resistance exercise, and the risk of metabolic diseases like CVD can be lowered [50]. This study showed that ageing significantly increased the levels of five TG species containing highly unsaturated acyl chains by as much as threefold with ageing, but exercise largely recovered their levels close to the levels in the young group. In accordance with the TG level, the fasting glucose level tended to decrease in exercise mice of the aged group (ESM Table S1). It is clear that individual TG levels significantly perturbed by ageing can be improved by physical exercise.

This study demonstrated the simultaneous analysis of FAs including HFAs, GPLs, SLs, and GLs using nUHPLC-ESI-MS/MS. This was used to elucidate the effect of exercise on variations in the plasma lipid profiles of mice against the ageing effect, which can be useful to understand the physiological influence of ageing on lipid perturbation in relation to many adult diseases and the physicochemical roles of physical exercise on lipidomic recovery against ageing-associated loss of physical status.

Authors' contributions K.U. Kim and J. C. Lee carried out the lipidomic analysis. K. J. Yoon and W. Lee performed animal experiments. H. Y. Moon designed the animal experiments. M.H. Moon supervised lipidomic analysis and wrote the manuscript. All of the authors discussed and approved the final manuscript.

Funding This study was funded by Korea Mouse Phenotyping project (NRF-2019M3A9D5A01102794) and in part by grants (NRF-2018R1A2A1A05019794 and NRF-2020R1C1C1006414) of the Ministry of Science, ICT & Future Planning through the National Research Foundation (NRF) of Korea.

Data availability The raw data that support the findings of this study are available in DataON (https://dataon.kisti.re.kr) at https://doi.org/10.22811/0101NC016738225011.0

Compliance with ethical standards

Conflict of interest The authors declare that they have no conflict of interest.

Ethical approval Animal experiments were approved by the Institutional Animal Care and Use Committee of Seoul National University (SNU-171226-3).

References

1. Langhammer B, Bergland A, Rydwik E. The importance of physical activity exercise among older people. Biomed Res Int. 2018;2018:7856823.
2. Valderrabano V, Steiger C. Treatment and prevention of osteoarthritis through exercise and sports. J Aging Res. 2010;2011:374653.
3. Donegan K, Fox N, Black N, Livingston G, Banerjee S, Burns A. Trends in diagnosis and treatment for people with dementia in the UK from 2005 to 2015: a longitudinal retrospective cohort study. Lancet Public Health. 2017;2(3):e149–e56.
4. Hoogeboom TJ, Dronkers JJ, Hulzebos EH, van Meeteren NL. Merits of exercise therapy before and after major surgery. Curr Opin Anaesthesiol. 2014;27(2):161–6.
5. Gruver AL, Hudson LL, Sempowski GD. Immunosenescence of ageing. J Pathol. 2007;211(2):144–56.
6. Deschenes MR. Effects of aging on muscle fibre type and size. Sports Med. 2004;34(12):809–24.
7. Wilson PW, Kannel WB. Obesity, diabetes, and risk of cardiovascular disease in the elderly. Am J Geriatr Cardiol. 2002;11(2):119–24.
8. Wenk MR. The emerging field of lipidomics. Nat Rev Drug Discov. 2005;4(7):594–610.
9. Bosio A, Binczek E, Stoffel W. Functional breakdown of the lipid bilayer of the myelin membrane in central and peripheral nervous system by disrupted galactocerebroside synthesis. Proc Natl Acad Sci U S A. 1996;93(23):13280–5.
10. Forouhi NG, Jenkinson G, Thomas EL, Mullick S, Mierisova S, Bhonsle U, et al. Relation of triglyceride stores in skeletal muscle cells to central obesity and insulin sensitivity in European and South Asian men. Diabetologia. 1999;42(8):932–5.
11. Goodpaster BH, Thaete FL, Simoneau JA, Kelley DE. Subcutaneous abdominal fat and thigh muscle composition predict insulin sensitivity independently of visceral fat. Diabetes. 1997;46(10):1579–85.
12. Rai S, Bhatnagar S. Novel lipidomic biomarkers in hyperlipidemia and cardiovascular diseases: an integrative biology analysis. Omics. 2017;21(3):132–42.
13. Brahma DK, Wahlang JB, Marak MD, Ch Sangma M. Adverse drug reactions in the elderly. J Pharmacol Pharmacother. 2013;4(2):91–4.
14. Mann S, Beedie C, Jimenez A. Differential effects of aerobic exercise, resistance training and combined exercise modalities on cholesterol and the lipid profile: review, synthesis and recommendations. Sports Med. 2014;44(2):211–21.
15. Kasumov T, Solomon TP, Hwang C, Huang H, Haus JM, Zhang R, et al. Improved insulin sensitivity after exercise training is linked to reduced plasma C14:0 ceramide in obesity and type 2 diabetes. Obesity (Silver Spring). 2015;23(7):1414–21.
16. Lipina C, Hundal HS. Lipid modulation of skeletal muscle mass and function. J Cachexia Sarcopenia Muscle. 2017;8(2):190–201.
17. Fahy E, Subramaniam S, Brown HA, Glass CK, Merrill AH Jr, Murphy RC, et al. A comprehensive classification system for lipids. J Lipid Res. 2005;46(5):839–61.
18. Shin TH, Kim HA, Jung JY, Baek WY, Lee HS, Park HJ, et al. Analysis of the free fatty acid metabolome in the plasma of patients with systemic lupus erythematosus and fever. Metabolomics. 2017;14(1):14.
19. Tan B, Liang Y, Yi L, Li H, Zhou Z, Ji X, et al. Identification of free fatty acids profiling of type 2 diabetes mellitus and exploring possible biomarkers by GC–MS coupled with chemometrics. Metabolomics. 2009;6(2):219–28.
20. Marmesat S, Velasco J, Dobarganes M. Quantitative determination of epoxy acids, keto acids and hydroxy acids formed in fats and oils at frying temperatures. J Chromatogr A. 2008;1211(1–2):129–34.
21. Tiuca I, Nagy K, Oprean R. Recent developments in fatty acids profile determination in biological samples - a review. Rev Rom Med Lab. 2015;23(4):371–84.

22. Chiu HH, Kuo CH. Gas chromatography-mass spectrometry-based analytical strategies for fatty acid analysis in biological samples. J Food Drug Anal. 2020;28(1):60–73.
23. Danne-Rasche N, Coman C, Ahrends R. Nano-LC/NSI MS refines lipidomics by enhancing lipid coverage, measurement sensitivity, and linear dynamic range. Anal Chem. 2018;90(13):8093–101.
24. Kim SH, Yang JS, Lee JC, Lee JY, Lee JY, Kim E, et al. Lipidomic alterations in lipoproteins of patients with mild cognitive impairment and Alzheimer's disease by asymmetrical flow field-flow fractionation and nanoflow ultrahigh performance liquid chromatography-tandem mass spectrometry. J Chromatogr A. 2018;1568:91–100.
25. Lee JC, Park SM, Kim IY, Sung H, Seong JK, Moon MH. High-fat diet-induced lipidome perturbations in the cortex, hippocampus, hypothalamus, and olfactory bulb of mice. Biochim Biophys Acta. 2018;1863(9):980–90.
26. Yang JS, Lee JC, Byeon SK, Rha KH, Moon MH. Size dependent lipidomic analysis of urinary exosomes from patients with prostate cancer by flow field-flow fractionation and nanoflow liquid chromatography-tandem mass spectrometry. Anal Chem. 2017;89(4):2488–96.
27. Byeon SK, Lee JY, Moon MH. Optimized extraction of phospholipids and lysophospholipids for nanoflow liquid chromatography-electrospray ionization-tandem mass spectrometry. Analyst. 2012;137(2):451–8.
28. Lim S, Byeon SK, Lee JY, Moon MH. Computational approach to structural identification of phospholipids using raw mass spectra from nanoflow liquid chromatography-electrospray ionization-tandem mass spectrometry. J Mass Spectrom. 2012;47(8):1004–14.
29. Yao C-H, Liu G-Y, Yang K, Gross RW, Patti GJ. Inaccurate quantitation of palmitate in metabolomics and isotope tracer studies due to plastics. Metabolomics. 2016;12(9):143.
30. Sindelar M, Patti GJ. Chemical discovery in the era of metabolomics. J Am Chem Soc. 2020;142(20):9097-105.
31. Semba RD, Zhang P, Adelnia F, Sun K, Gonzalez-Freire M, Salem N Jr, et al. Low plasma lysophosphatidylcholines are associated with impaired mitochondrial oxidative capacity in adults in the Baltimore longitudinal study of aging. Aging Cell. 2019;18(2):e12915.
32. Moaddel R, Fabbri E, Khadeer MA, Carlson OD, Gonzalez-Freire M, Zhang P, et al. Plasma biomarkers of poor muscle quality in older men and women from the Baltimore longitudinal study of aging. J Gerontol A Biol Sci Med Sci. 2016;71(10):1266–72.
33. Kim S, Cheon H-S, Song J-C, Yun S-M, Park SI, Jeon J-P. Aging-related changes in mouse serum glycerophospholipid profiles. Osong Public Health Res Perspect. 2014;5(6):345–50.
34. De Guzman JM, Ku G, Fahey R, Youm Y-H, Kass I, Ingram DK, et al. Chronic caloric restriction partially protects against age-related alteration in serum metabolome. Age. 2013;35(4):1091–104.
35. Razquin C, Toledo E, Clish CB, Ruiz-Canela M, Dennis C, Corella D, et al. Plasma lipidomic profiling and risk of type 2 diabetes in the PREDIMED trial. Diabetes Care. 2018;41(12):2617–24.
36. Farag KA, Mostafa MB, Sheta EM, Fetaih HA. Ameloblastoma (adamantinoma) in a buffalo. Zentralbl Veterinarmed A. 1993;40(6):422–6.
37. Ryu SB, Karlsson BH, Ozgen M, Palta JP. Inhibition of phospholipase D by lysophosphatidylethanolamine, a lipid-derived senescence retardant. Proc Natl Acad Sci U S A. 1997;94(23):12717–21.
38. Meylaers K, Clynen E, Daloze D, DeLoof A, Schoofs L. Identification of 1-lysophosphatidylethanolamine (C(16:1)) as an antimicrobial compound in the housefly, *Musca domestica*. Insect Biochem Mol Biol. 2004;34(1):43–9.
39. Dohi T, Miyauchi K, Ohkawa R, Nakamura K, Kishimoto T, Miyazaki T, et al. Increased circulating plasma lysophosphatidic acid in patients with acute coronary syndrome. Clin Chim Acta. 2012;413(1–2):207–12.
40. Simms AD, Batin PD, Kurian J, Durham N, Gale CP. Acute coronary syndromes: an old age problem. J Geriatr Cardiol. 2012;9(2):192–6.
41. Pararasa C, Ikwuobe J, Shigdar S, Boukouvalas A, Nabney IT, Brown JE, et al. Age-associated changes in long-chain fatty acid profile during healthy aging promote pro-inflammatory monocyte polarization via PPAR γ. Aging Cell. 2016;15(1):128–39.
42. Pararasa C, Bailey CJ, Griffiths HR. Ageing, adipose tissue, fatty acids and inflammation. Biogerontology. 2015;16(2):235–48.
43. Keane DC, Takahashi HK, Dhayal S, Morgan NG, Curi R, Newsholme P. Arachidonic acid actions on functional integrity and attenuation of the negative effects of palmitic acid in a clonal pancreatic beta-cell line. Clin Sci (Lond). 2011;120(5):195–206.
44. Oh YS, Bae GD, Baek DJ, Park EY, Jun HS. Fatty acid-induced lipotoxicity in pancreatic beta-cells during development of type 2 diabetes. Front Endocrinol (Lausanne). 2018;9:384.
45. Chen C-Y, Lee C-W, Chien S-C, Su M-I, Lin S-I, Cheng C-W, et al. Dyslipidemia management for elderly people with metabolic syndrome: a mini-review. Int J Gerontol. 2018;12(1):7–11.
46. Menahan LA. Age-related changes in lipid and carbohydrate metabolism of the genetically obese mouse. Metabolism. 1983;32(2):172–8.
47. HASKELL WL. The influence of exercise training on plasma lipids and lipoproteins in health and disease. Acta Med Scand. 1986;220(S711):25–37.
48. Sady SP, Thompson PD, Cullinane EM, Kantor MA, Domagala E, Herbert PN. Prolonged exercise augments plasma triglyceride clearance. Jama. 1986;256(18):2552–5.
49. Lu C-W, Yang K-C, Chang H-H, Lee L-T, Chen C-Y, Huang K-C. Sarcopenic obesity is closely associated with metabolic syndrome. Obes Res Clin Pract. 2013;7(4):e301–e7.
50. Dieli-Conwright CM, Courneya KS, Demark-Wahnefried W, Sami N, Lee K, Buchanan TA, et al. Effects of aerobic and resistance exercise on metabolic syndrome, sarcopenic obesity, and circulating biomarkers in overweight or obese survivors of breast cancer: a randomized controlled trial. J Clin Oncol. 2018;36(9):875.